



1 **The weather of 1740, the coldest year in Central Europe in 600 years**

2

3 Stefan Brönnimann^{1,2,*}, Janusz Filipiak³, Siyu Chen^{1,2}, and Lucas Pfister^{1,2}

4 ¹*Oeschger Centre for Climate Change Research, University of Bern, Bern, Switzerland*

5 ²*Institute of Geography, University of Bern, Bern, Switzerland*

6 ³*Department of Physical Oceanography and Climate Research, University of Gdansk, Gdansk, Poland*

7

8 *corresponding author: Stefan Brönnimann, stefan.broennimann@giub.unibe.ch

9

10

11 **Abstract**

12 The winter 1739/40 is known as one of the coldest winters in Europe since early instrumental measurements
13 began. Many contemporary sources discuss the cold waves and compare the winter to that of 1708/09. It is less
14 well known that the year 1740 remained cold until August and again in October, and that negative temperature
15 anomalies are also found over Eurasia and North America. The 1737/40 cold season over northern midlatitude
16 land areas was perhaps the coldest in 300 years, and 1740 was the coldest year in Central Europe in 600 years.
17 New monthly, global climate reconstructions allow addressing this momentous event in greater detail, while
18 daily observations and weather reconstructions give insight into the synoptic situations. Over Europe, we find
19 that the event was initiated by a strong Scandinavian blocking in early January, allowing the advection
20 continental cold air. From February until June, high pressure dominated over Ireland, arguably associated with
21 frequent East Atlantic blocking. This led to cold air advection from the cold northern North Atlantic. During the
22 summer, cyclonic weather dominated over Central Europe, associated with cold and wet air from the Atlantic.
23 The possible role of oceanic influences (El Niño) and external forcings (eruption of Mount Tarumae in 1739)
24 are discussed. While a possible El Niño event might have contributed to the winter cold spells, the East Atlantic
25 blocking is arguably unrelated to either El Niño or the volcanic eruption. In all, the cold year of 1740 marks one
26 of the strongest, arguably unforced excursions in European temperature.

27

28 **Introduction**

29 The winter 1739/40 is known as an extremely cold winter in Central Europe, rivalling the winter of
30 1708/09 as the coldest in the past several hundred years. The winter was severe across Europe,
31 including Switzerland (Pfister and Wanner, 2021), Poland (Filipiak et al., 2019), the British Isles
32 (Manley, 1957; Lamb 1967), Netherlands and Germany (Jones and Briffa, 2006) and other regions.
33 The winter started early, already in October 1739 and ended only in June 1740, and it is particularly
34 well known for frozen rivers and ice floods. Filipiak et al. (2019) reported that after unusually cold
35 easterly winds in mid-October 1739 at the coast of the Baltic Sea, there were very heavy snowfalls
36 and several waves of severe frost in November 1739, January 1740 and again in February and March,
37 with the most extreme conditions in January 1740. The coastal waters of the Baltic Sea and
38 particularly the Vistula River were frozen until mid-April with the ice thickness exceeding 50 cm.



39 Water from the huge amounts of snow melting in April caused a large and long-lasting flood in the
40 Baltic lowlands. In Ireland, the intense cold lasted for weeks, interspersed with only short break of
41 slight thaw (Gillespie, 1939). Potatoes and turnips were destroyed, cattle and even fish died (Dickson,
42 1997). Among the consequences was the Irish famine of 1740/41 (Engler et al., 2013). However, the
43 winter was only the start of a series of adverse weather and climate events, which led to high mortality
44 and high cereal prices also in Central Europe (Post, 1984). Due to the frozen rivers and long-term
45 shutdown of mills in Poland there was even a shortage of bread, and the administrative authorities of
46 many cities started to provide food, wood and means of subsistence to the poorest people (Filipiak et
47 al. 2019). Jones and Briffa (2006) pointed out that the entire year 1740 was cold and that it
48 particularly contrasted with the warm 1730s.

49 Reconstructions of sea-level pressure have allowed characterising the anomalies atmospheric
50 circulation of this specific period in a bit more detail. Jones and Briffa (2006), using hand analysed
51 monthly sea-level pressure fields, noted that in winter, the Icelandic Low and the Azores High were
52 weaker than normal and the dominant feature was a continental or Scandinavian High. Engel et al.
53 (2013), using sea-level pressure and 500 hPa geopotential height reconstruction of Luterbacher et al.
54 (2002), additionally found a strong high-pressure situation in spring 1740, resembling a negative
55 phase of the East Atlantic pattern and leading to cold air advection from the northwest.

56 It is less well known, however, that the winter 1739/40 was not only cold in Europe but also in North
57 America and parts of Asia. A cold season (Oct-May) temperature field reconstruction for midlatitude
58 (35-70° N) land areas from 1701-2020 indicates that this might have been the coldest cold season of
59 the last 300 years (Reichen et al. 2022). Recently, a comprehensive, global 3-dimensional climate
60 reconstruction was published (Valler et al., 2024) and numerous additional meteorological time series
61 have been digitised such that we can now study this event in more detail and on the daily scale, i.e.,
62 the scale of the weather events.

63 Here we study the weather of the year of 1740 using the new reconstructions combined with daily
64 meteorological series. We analyse sequence of events on monthly scale, zoom into prominent cold air
65 outbreaks on daily scale, and analyse role of forcings and large-scale circulation mechanisms.

66

67 **Data and Methods**

68 *Reconstructions*

69 We use the ModE-RA (Modern Era Reanalysis) family of reconstructions (Valler et al., 2024), which
70 provide monthly, global 3-dimensional fields back to 1421. Similar as the precursor product
71 EKF400v2 (Valler et al., 2022), ModE-RA is based on the offline assimilation of a large amount of
72 natural proxies, documentary data, and instrumental observations into an ensemble of 20 atmospheric
73 model simulations (ModE-Sim, Hand et al., 2023). Another product, termed ModE-RAclim, was



74 generated by assimilating the same observations into a sample of 100 realisations, randomly drawn
75 from all members and all model years of ModE-Sim. Analysing ModE-Sim and ModE-RAclim along
76 with ModE-RA allows to disentangle the role of forcings and observations. ModE-Sim was forced by
77 monthly sea-surface temperatures (Samakinwa et al., 2021, Titchner and Rayner, 2014), volcanic,
78 land-surface and solar forcings following the PMIP4 protocol (Jungclaus et al., 2017). It does not see
79 the assimilated observations but only the model boundary conditions. In contrast, ModE-RAclim does
80 not see the time-dependent boundary conditions, but only the observations. We performed the
81 analyses on the individual ensemble members, but when plotting spatial fields we show the ensemble
82 mean only. When plotting anomalies these were expressed relative to the 30 preceding years (1710-
83 39). Note that the ModE-RA data set was constructed as anomalies from a 71-yr moving average,
84 therefore the last three decades of the data set are less well constrained.

85 For comparison, we also used the reconstruction XBRWccc (Reichen et al., 2022), which provides
86 cold season (May-Oct) temperature field reconstructions for the northern extratropics. It is based on a
87 Bayesian reweighting approach of model simulations that are very similar as ModE-Sim. Only
88 phenological data (mostly ice phenology, i.e., the freezing and thawing dates of rivers and lakes, some
89 plant phenological data) are used to constrain this reconstruction.

90 *Meteorological series*

91 In this paper we work with daily meteorological time series from measurements and observations,
92 which were inventoried in Brönnimann et al. (2019) and compiled in Lundstad et al. (2022). These
93 compilations are complemented with additional series. Table 1 gives an overview of the series used
94 and their sources.

95 For some of the analyses, all segments were deseasonalized by fitting and subtracting the first two
96 harmonics of the annual cycle and then standardized. This allows for better comparison of series with
97 different numbers of observations per day and allows including series on unknown scales (such as
98 temperature in Berlin). Note that a unique reference period that works for all series does not exist. If
99 possible we used 1731-50, but several of the segments were too short (in once case slightly longer;
100 following in existing segment). This reference is shorter than that for ModE-RA (analyses of the two
101 data sets are performed separately). For the special case of Montpellier, where we have very irregular
102 data (but which always include the monthly minima and maxima), we proceeded in the same way for
103 the deseasonalizing. However, because the series consists mostly of maxima and minima, it has a
104 standard deviation that is ca. 1.5-2 times larger than that at other stations. Therefore, we inflated the
105 standardized anomalies by 1.5.

106



107 **Table 1.** Locations and sources of daily weather data used in this study, variables (Var., p = pressure, mslp =
108 mean sea-level pressure, T = temperature, dir = wind direction, RR = precipitation, wn = weather notes), period
109 and source

Location	Var.	Period	Source
Haarlem	T	1735-42	KNMI
Leiden	T, p	1740-50	KNMI
London	mslp	1731-50	Cornes et al., 2012, 2023
Montpellier	(T, p)*	1738-48	Lundstad et al., 2022
Paris	T	1732-57	Rousseau 2019
Versailles	wn		Société Météorologique de France, 1866
Berlin	T, p	1738-43	Brönnimann and Brugnara, 2023
Gdansk	T, p, wn	1740	Filipiak et al., 2019
Nuremberg	p, dir	1732-43	Brönnimann and Brugnara, 2023
Uppsala	T, mslp	1731-50	Bergström and Moberg, 2002
Padova	mslp, RR	1731-50	Camuffo and Jones 2002
Bologna	T	1731-50	Camuffo and Jones 2002
Channel	dir	1731-50	Barriopedro et al. 2014
St. Blaise	(dir), wn		Pfister et al. 2017

110 * pressure was only used until April 1746, morning (typically 3-8 AM) and afternoon (mostly 3 PM) were treated separately.

111 In addition to the instrumental series, we also consulted weather diaries and other historical sources to
112 better characterize the weather of 1740. This includes observations from Gdansk (Filipiak et al.,
113 2019), Berlin (Brönnimann and Brugnara, 2023), Versailles (Société Météorologique de France,
114 1866), and St. Blaise (from EURO-CLIMHIST, Pfister et al., 2017). Note that most of these series
115 were assimilated in ModE-RA.

116 *Daily reconstructions of sea-level pressure fields*

117 For the analyses of daily weather, we not only used the raw data, but reconstructed daily pressure
118 fields over Europe from the pressure observations using a simple analog approach (see also Pappert et
119 al., 2022). For that we used the ERA5 reanalysis (Hersbach et al., 2020) from 1940-2023. We
120 extracted sea-level pressure at the 1740 observation locations, deseasonalized and standardized the
121 data in the same way as described above (using the entire period) and then determined, for each day in
122 1740, the closest analog day in ERA5 within a window of ± 60 calendar days of the target day. We
123 used the Euclidian distance as a distance measure. Once the closest analog is found, the sea-level
124 pressure field for that day is taken as the reconstruction, without any further postprocessing.

125 An evaluation was performed by applying the procedure to the year 1940 within ERA5 using 1941-
126 2023 as pool of analogs. Comparing the results against the actual fields in 1940 (Fig. S1) shows
127 excellent correlations and a low root-mean squared error over central Europe, but a rapid deterioration
128 towards the Southwest and Northeast.

129 *Index time series*

130 In addition to spatial analyses and analyses of the instrumental series, we also calculated time series
131 within ModE-RA. We defined Central European temperature as the average 2 m temperature in the



132 region 5-25° E, 45-55° N. The index was also calculated in the CRUTEM5 data set (Osborn et al.,
133 2021) in order to extend the reconstruction to the present. Furthermore, we calculated indices for the
134 North Atlantic Oscillation (NAO) and the East Atlantic Pattern (EA). The former was defined as the
135 sea-level pressure difference between the locations of Lisbon and Gibraltar. For the latter, different
136 definitions exist. We use the sea-level pressure difference between 30° E/45° N and 20° W/55° N,
137 which is similar to Barneston and Livezey (1987) and denoted EA1 in the following. We also define
138 an index EA2 as the difference between 30° E/55° N and 20° W/55° N, which is more similar to the
139 definition of Wallace and Gutzler (1981). Note that in all indices, only the difference was calculated
140 and no standardization was used, since the standard deviation in the ModE-RA datasets changes over
141 time. We mostly analyse Jan-Feb for NAO and Mar-May for EA1 and EA2.

142 Finally, we also used a NINO3.4 index (Sep-Feb) which we calculated from ModE-RA 2 m
143 temperature data. For addressing the volcanic forcing, we used the estimated radiative forcings for
144 different volcanic eruptions as given in Sigl et al. (2015). We selected eruptions with a global forcing
145 stronger than -2 W m^{-2} . For both NINO3.4 and volcanic years, we analysed the NAO and EA indices
146 of the subsequent winter and spring periods. For NINO3.4 we used a correlation analyses, for
147 volcanic eruptions compositing.

148

149 **Results**

150 *Descriptions of the weather and impacts in Europe*

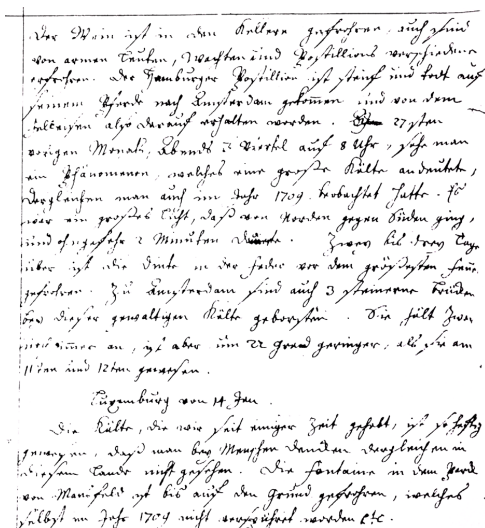
151 The low temperatures in the winter 1739/40 and the consequences are well documented across
152 Europe. Here we present the weather information from the three locations listed in Table 1.
153 Interestingly, the winter 1740 was compared with the winter of 1709, which was still in the memory
154 of the people at that time, in several of the sources. As an example, Fig. 1 shows an excerpt of a
155 weather diary led by Christine Kirch (Brönnimann and Brugnara, 2023). The text, spanning a travel
156 from Paris to Luxembourg, speaks of freezing wine, fountains freezing to the ground, and bursting
157 bridges. At several instances it compares measured temperatures with those in 1709 and finds that
158 1740 temperatures were even lower.

159 Commissaire Narbonne noted the weather in Versailles from 1709-45 (Société Météorologique de
160 France, 1866). According to his notes, the Seine was frozen, and public fires were lit in the streets of
161 Paris from 9 Jan to 9 Feb 1740 and similarly in Versailles. Severe frost is noted in January, February
162 and March. Low temperatures are noted throughout the year. On 7-8 October, during grape harvest,
163 Versailles experienced a severe frost and grapes were frozen.

164 According to two prominent scientists of Gdansk at the Baltic Sea coast, Northern Poland – Michael
165 Christian Hanov (a pioneer of systematic instrumental measurements in the city) and Gottfried Reyger
166 (botanist and chronicler), a winter of 1740 in Gdansk was unprecedented (Filipiak et al. 2019). Hanov



167 recorded the lowest temperatures between 8th and 14th January, 1740 with a minimum on the morning
168 of the 10th January. Further, extreme cold occurred also between 1st and 7th February, 17th and 25th
169 February and in a few selected days in March. Reyger compared several severe winters in the 18th
170 century (1709, 1729, 1740 and 1784) and pointed out that winter of 1740 was undoubtedly the coldest
171 one, however in 1709 the duration of severe frost was even higher. Harsh weather conditions during
172 winter and a late and cool spring resulted in a very late appearance of vegetation – species usually
173 present in early March were observed only in the last days of April. Although the ice on the Baltic Sea
174 and the Vistula remained longer in April 1771 and 1784 than in 1740, the flood lasting many weeks
175 had a significant impact on the economy in 1740. Both researchers noticed unnatural behaviour of
176 animals and numerous cases of animals freezing, both farm animals and wild ones. Among the
177 increased number of human diseases, many frostbites were noticed, but the mortality rate did not
178 increase noticeably. Further, Hanov pointed out an exceptionally cold May with extremely cloudy
179 conditions (whereas a cloudiness is usually minimum in May in the annual course), fog and snow
180 constantly present even at the end of the month, several frosts in June and unusual weather conditions
181 during summer. The harvest, delayed by a cold and wet August, took place in an exceptionally sunny
182 and warm September (according to Reyger it was “the best weather in the whole year”), the autumn
183 fruit harvest was also very good. October was cold again in Gdansk. The first snowfall occurred
184 already on the 5th. Hanov also reported the anomalously cold weather in selected months of 1740
185 (particularly in January) in other cities in Europe, i.e., Königsberg, Hamburg, Kiel, Wittenberg, the
186 Hague, Uppsala and Petersburg.



187
188 **Fig. 1.** Excerpt of “Kirch diary” led by Christine Kirch for 13 and 14 January 1740 (see Brönnimann and
189 Brugnara, 2023).

190 In Switzerland, a detailed weather diary is available from the vine-grower family Péter from St.
191 Blaise. The diary notes the very low temperature from 8-12 January, which are followed by warmer



192 weather. However, all of February then was described as “very cold” in St. Blaise. In February and
193 March, water bodies were frozen and navigation stopped on Lake Biel and Lake Morat, and this
194 continued into April (19 Apr, parts of Lake Neuchatel were frozen). Most of March the weather diary
195 notes “frost”. Frost impact on grapevines was reported in April and May. Snowfall was observed until
196 8 May (at low elevations) and 20 May (at higher elevations).

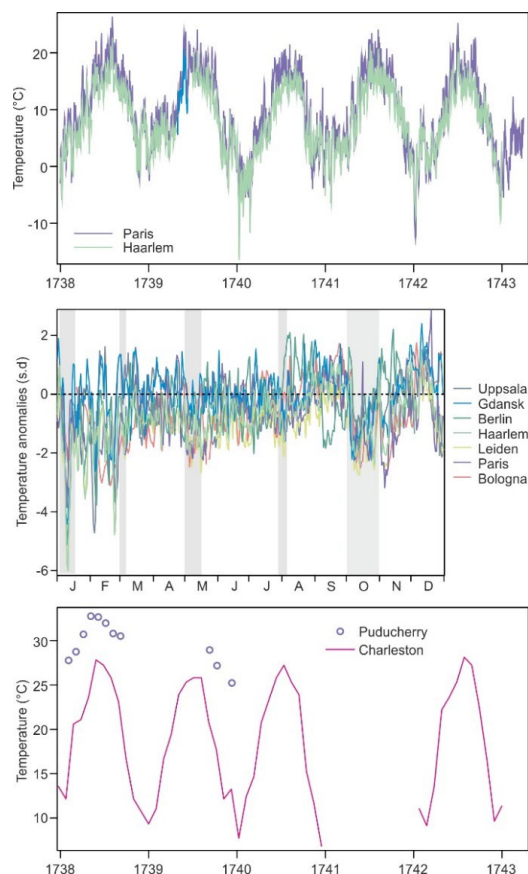
197 *Instrumental measurements*

198 For the year 1740, eight daily temperature series are available, although Montpellier is very sporadic
199 and Haarlem and Leiden are very close. More series would exist, but are not available in daily,
200 digitised format (see Brönnimann et al., 2019). As an example, Fig. 2 (top) shows the raw daily mean
201 temperature series from Paris and Haarlem from 1738–43. The low temperatures in the winter 1739/40
202 clearly stand out, and it becomes visually apparent that also the other seasons were colder than the
203 other years shown (the winter 1741/42 also is very cold). The winter 1739/40 began early, with low
204 temperatures in October and November 1739. After a warm December, temperatures then dropped in
205 January. Low temperatures lasted consistently until August, and October and November were again
206 very cold.

207 After deseasonalizing and standardizing the series (Fig. 2, middle), it can be seen that temperatures
208 were below average (1731–1750, where possible) at most stations during most of the year. Only
209 August and September had warm intervals. In the following we discuss several episodes (marked with
210 grey bars) in more detail by analysing the daily series (Fig. 3) and pressure fields (Fig. 4).

211 One of the most severe cold spells occurred in the first half of Jan 1740. It peaked at 10–11 Jan and
212 brought very low temperatures to Western Europe, up to 6 standard deviations below the mean, which
213 is extraordinary (Fig. 3). The cold was not so intense in the North and South, i.e., in Uppsala and
214 Bologna (although temperature also fell below -2 standard deviations at those locations). Temperature
215 remained low also during the rest of the month, with a similar pattern. Pressure was below normal in
216 the South and above normal in the North; the gradient in the standardized anomalies persisted during
217 the entire month. The distinct pressure drop in Padova on 27 Jan is suspect and could be outlier, but
218 also Montpellier shows a pressure drop.

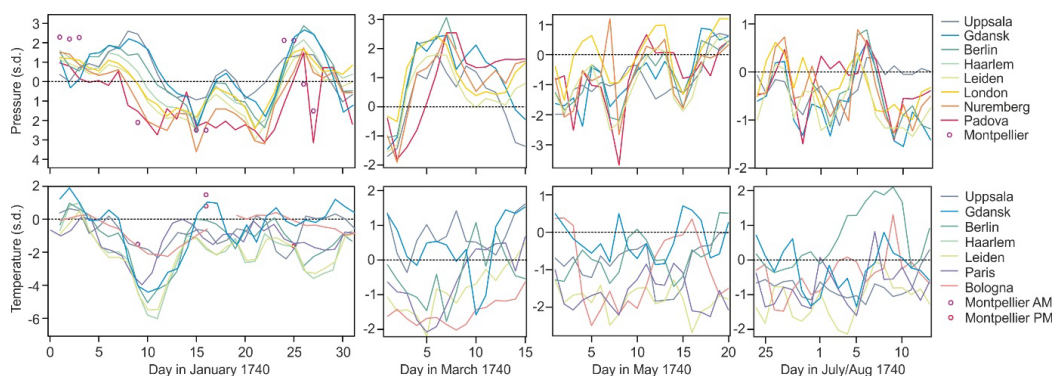
219 In early March 1740, negative temperature anomalies were observed in the South and West, though
220 not nearly as strong as in the January case. All stations show a very strong pressure increase from
221 strong negative anomalies to very high positive anomalies that persisted for 10 days. The third cold
222 period, in May 1740, was less homogeneous. Again, temperatures were persistently low in Western
223 Europe (Paris, Leiden), only slightly below normal in Gdansk and Uppsala. Temperatures were also
224 low in Bologna the beginning of the month and again towards 20 May. Pressure was generally below
225 normal, but above in London.



226

227 **Fig. 2.** (top) Daily temperature series from two selected European stations from 1738-43, (middle) standardized
 228 daily temperature anomaly at seven European sites in 1740 and (bottom) the only two available non-European
 229 temperature series that cover the boreal winter 1739/40. Shaded bars in the middle panel denote the periods
 230 chosen for more detailed analysis.

231



232

233 **Fig. 3.** Standardized temperature and sea-level pressure anomaly series for the four episodes 1-31 Jan, 1-15 Mar,
 234 1-20 May, and 24 Jul to 14 Aug 1740.



235 The fourth chosen episode featured below normal temperature at most stations. An exception is
236 Berlin, where temperatures exceeded 2 standard deviations. This appears suspicious, but we have no
237 indications that could lead us to remove the data. Pressure was mostly below normal. Padova and
238 Uppsala show sometimes a different behaviour whereas all other stations run in parallel. Overall,
239 analysing the long pressure time series from London or Uppsala, the year 1740 did not feature
240 particularly many extreme days.

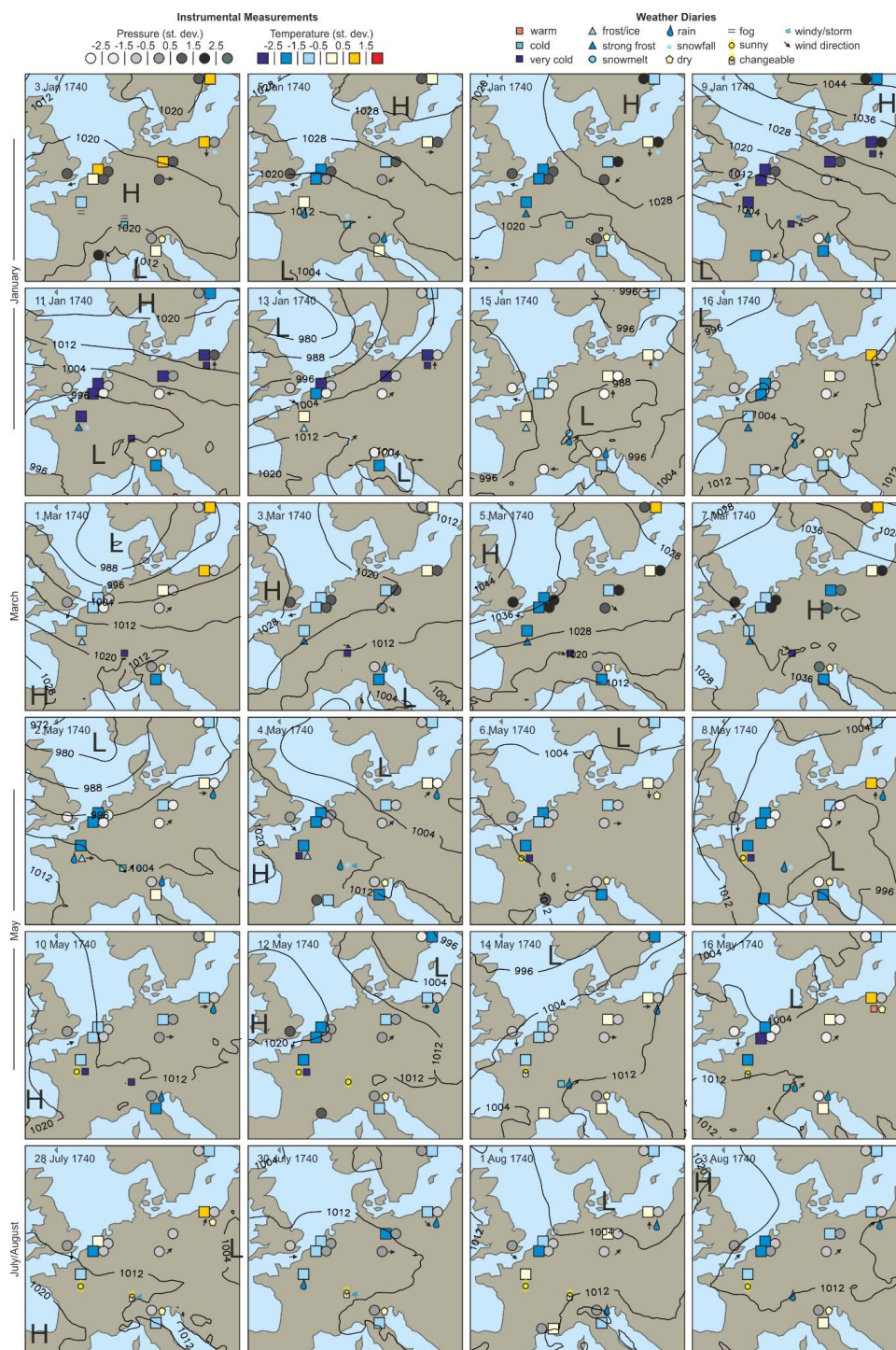
241 *Weather maps*

242 Plotting the daily data on a map, along with the weather observations and the analog pressure
243 reconstructions allows an inspection of the pressure systems and of the flow over central Europe.
244 During the cold spell in January (Fig. 4, top), a strong high-pressure system established over
245 Scandinavia, and at the same time a rather strong low pressure system developed over the northern
246 Mediterranean, causing a strong inverse pressure gradient across Europe. This situation can firmly be
247 addressed as a Scandinavian blocking event, allowing cold, continental air to flow in from the east.
248 The main spell lasted only five days, but further similarly extreme cold spells occurred in January and
249 February. In the latter cases, positive pressure anomalies were strongest over London, but stretching
250 into Scandinavia (not shown). Note that the sea-level pressure maps are based only on pressure
251 observations and are independent of temperature and wind observations.

252 In the first half of March, pressure was high everywhere and temperatures were below normal
253 everywhere except at Uppsala. Figure 4 depicts the beginning of this high-pressure period. After a
254 strong low-pressure situation, pressure began to build up in the West (UK) and then established over
255 the continent. The strongest pressure anomalies were observed first in Gdansk and Berlin. Again,
256 continental Europe was in an easterly flow, bringing relatively (though not extremely) cold
257 continental air to Central and Western Europe.

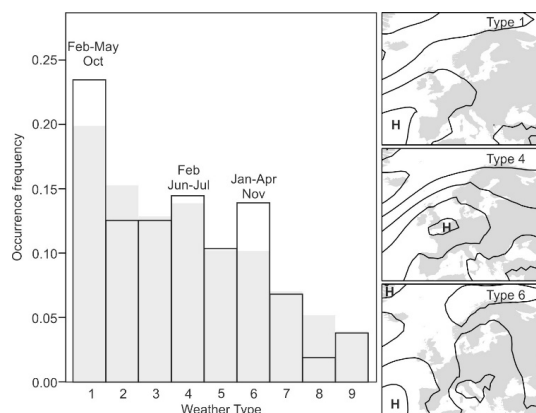
258 The generally low temperatures in 1740 not only included sharp but temporally limited drops of
259 temperature due to cold spells, but also longer, persistent phases of below normal temperature. An
260 example is the third selected period in May 1740. During this period, pressure was relatively low over
261 continental Europe and arguably higher over England. The monthly mean reconstruction shows a
262 strong East Atlantic pattern throughout spring. Frequent westerly or northwesterly wind arguably
263 brought cold air from the northern North Atlantic, which at that time of the year is very cold relative
264 to the land. Finally, the lowest row in Fig. 4 shows a situation in late July and early August. It was
265 rather cold and rainy, with typical cyclonic weather dominating. The fifth period noted in Fig. 2 is the
266 month of October, which was persistently cold at most stations and which will be analysed in the
267 following based on monthly charts.

268



269

270 **Fig. 4.** Standardized anomalies of pressure and temperature as well as weather observations at stations and
 271 analog sea-level pressure reconstruction (hPa) for four selected periods in Jan, Mar, May, and Jul/Aug 1740.



272

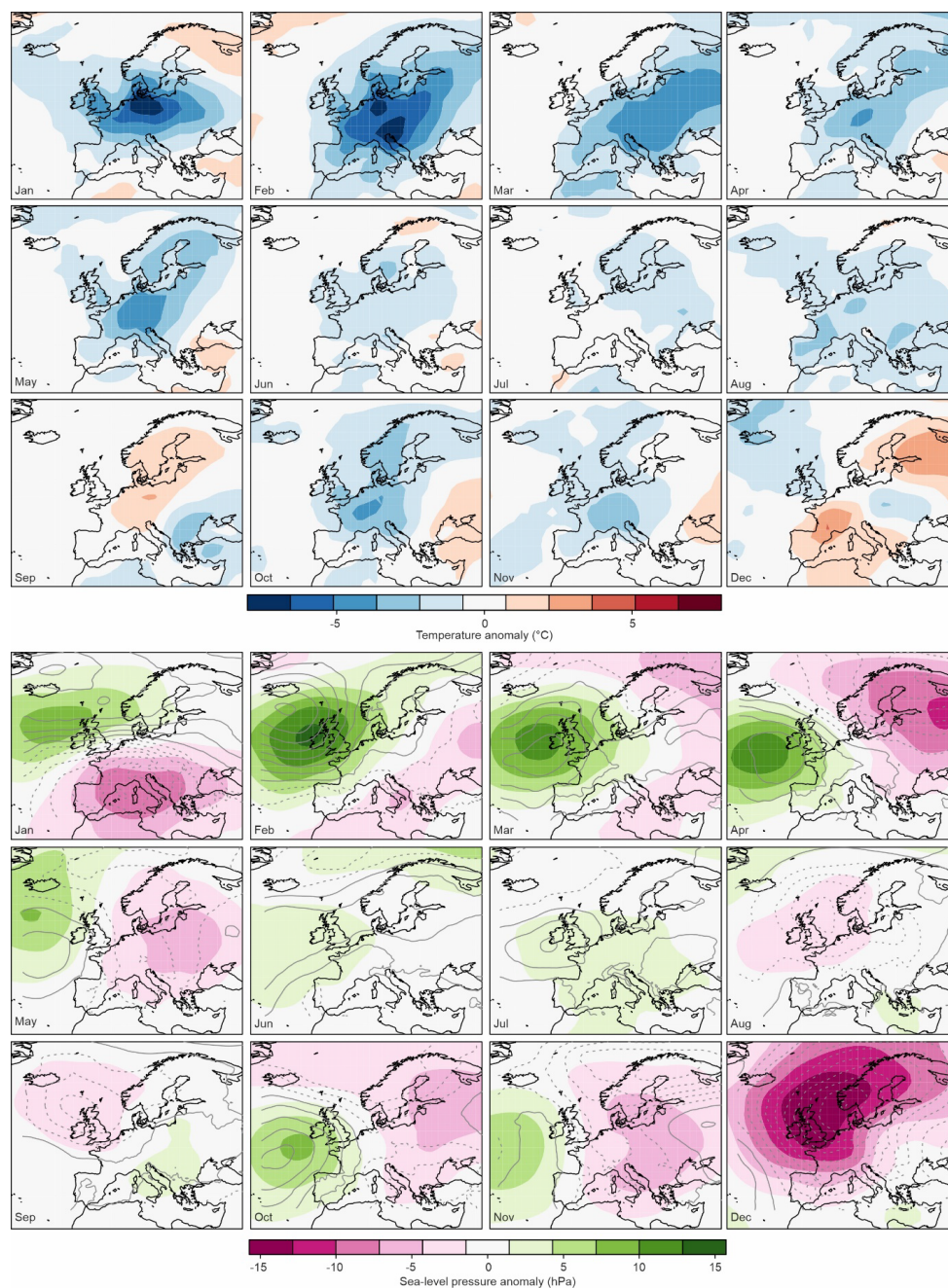
273 **Fig. 5.** Frequency of daily weather types in the CAP9 classification in 1740 (open rectangles)
274 1991-2020 (grey). Right insets show the composite fields for sea-level pressure for types 1, 4, and 6,
275 respectively, in 1940-2020 from ERA5.

276 Before focusing on monthly charts, though, we would like to analyse how the daily sea-level pressure
277 maps translate into monthly means. For this we analysed the frequency of daily weather types over
278 central Europe, specifically the CAP9 (Cluster Analysis of Principal Components with 9 types)
279 classification that reaches back to 1728 (Pfister et al., 2024). Three weather types were clearly
280 overrepresented in that year, namely 1, 6, and to a lesser extent 4. These patterns (displayed in Fig. 5,
281 right) are mostly types with high pressure systems over Western Europe.

282 We now turn to the analysis of monthly anomaly fields in the ModE-RA data sets (Fig. 6, see Fig. S2
283 for monthly anomaly fields from Oct-Dec 1739) and specifically the fields for October. Temperature
284 anomalies in this month were negative in Central Europe. Although they were not as strong as during
285 the winter months January to March, they reached down to -4°C which is remarkable for this time of
286 the year. As noted earlier, severe frost was observed in Versailles such that the grapes froze.

287 In ModE-RA we can also analyse monthly anomaly fields of sea-level pressure (Fig. 6, bottom, fields
288 for Oct-Dec 1739 are shown in Fig. S2). From January into June and then again in October and
289 November we find positive sea-level pressure anomalies in the East Atlantic and negative over
290 Eastern Europe. This is similar to the East Atlantic Pattern, which we will address in the following.
291 The positive anomalies could point to more frequent blocking situations. In Fig. 4 (top) we have
292 addressed Scandinavian blocking for the cold spell in January. However, this is not seen in the
293 monthly average, where the core of the positive anomaly is situated further in the West. The pattern
294 resemble more a negative North Atlantic Oscillation index, although the anomaly centres are shifted
295 southeastward.

296



297

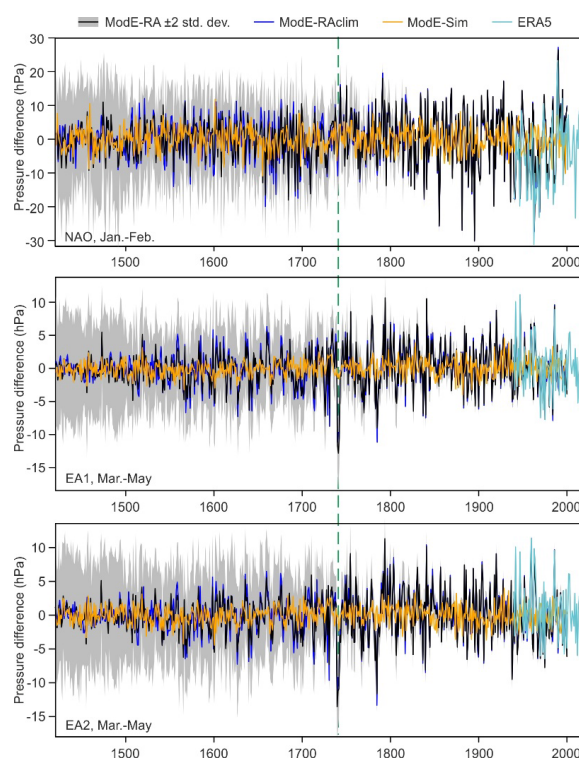
298 **Fig. 6.** Monthly anomalies (with respect to 1710-39) of (top) temperature and (bottom) sea-level pressure in
299 1740 in the ModE-RA ensemble mean. The bottom figure also shows sea-level pressure anomalies from the
300 analog approach (relative to 1991-2020, contour distance 2 hPa centred around zero, negative dashed).

301 We calculated indices for the NAO for January and February and for the East Atlantic pattern for

302 March to May for all three ModE products (Fig. 7, the ensemble spread is only shown for the ModE-



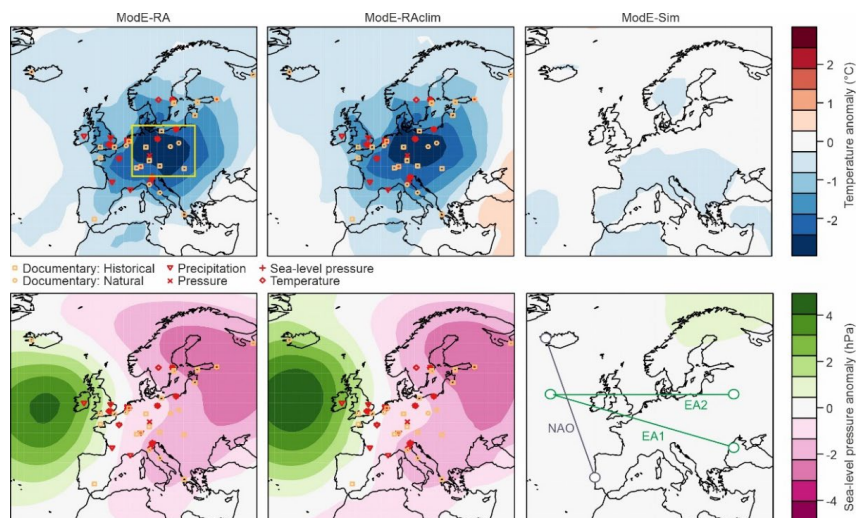
303 RA for better visualisation). In ModE-RA and ModE-RAclim, which are very similar, the NAO was
304 negative in 1740, but it was by no means an extreme year. However, the negative East Atlantic pattern
305 in spring is unique in the entire record since 1421, both for EA1 and EA2 (very similar results are
306 found in the annual mean). The analysis of ModE-Sim shows that only a small part of the variability
307 is reproduced purely from the model boundary conditions, which means that presumably the forced
308 component of the signal is relatively small at least in ModE-Sim. In order to extend the series to the
309 present we also calculated the indices in ERA5 (using 1991-2020 as a reference, correlations in the
310 overlapping period for NAO, EA1, and EA2 are 0.992, 0.936, 0.949, respectively). Neither of the
311 series shows a trend, neither in ModE-RA nor in ERA5. Also, no clear change in variability is seen in
312 ModE-RA, although the recent variability in the NAO in ERA5 is very large in a 600 year context.



313
314 **Fig. 7.** Indices of the NAO Index in Jan-Feb and of the EA1 and EA2 in Mar-May relative to 1710-39. Shown
315 are the three data sets ModE-RA (grey shading denotes ± 2 standard deviations of the ensemble), ModE-RAclim
316 and ModE-Sim as well as ERA5. The green dashed line marks the year 1740.
317 An interesting aspect in the monthly analysis is the persistence even at a seasonal and longer time
318 scale. In particular, the East Atlantic pattern is persistent or recurring. We therefore also analysed the
319 annual mean fields of temperature and pressure anomalies (Fig. 8). Again, ModE-RA and ModE-
320 RAclim show very similar patterns. For temperature, the ModE-Sim shows negative temperature
321 anomalies of up to 0.5 °C over parts of Europe, hence there is a contribution of boundary conditions



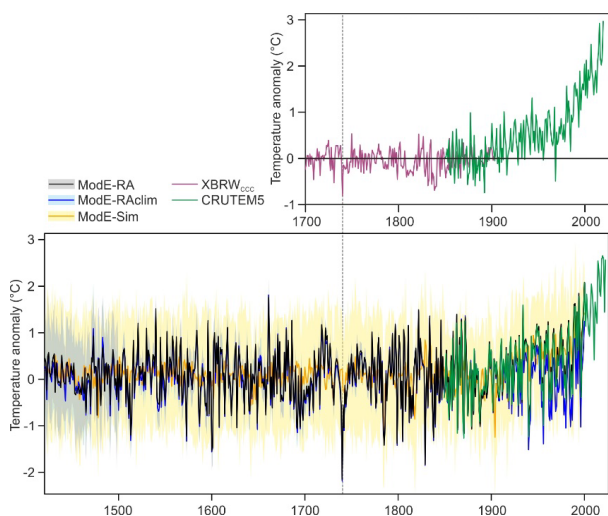
322 on a large scale, though much weaker than the full reconstruction. For sea-level pressure, there is no
 323 contribution from ModE-Sim. The pattern in the annual mean sea-level pressure anomaly is more
 324 similar to the East Atlantic pattern of Wallace and Gutzler (1981) rather than the corresponding
 325 pattern in Barneston and Livezey (1987).



326

327 **Fig. 8.** Annual mean anomalies of (top) temperature and (bottom) sea-level pressure in 1740 in (left) ModE-RA,
 328 (middle) ModE-RAclim, and (right) ModE-Sim. Also shown are the location and types of observations for Oct
 329 1739-Mar 1740 on which ModE-RA and ModE-RAclim are based. The yellow rectangle(top left) shows the
 330 region defined as Central Europe. The bottom right figure shows the definition of NAO and EA indices.

331



332

333 **Fig. 9.** Top: Time series of cold season (May-Oct) mean temperature over northern extratropical (35-70° N)
 334 land areas. Bottom: Time series of annual mean, Central European temperature in the three reconstructions
 335 ModE-RA, ModE-RAclim, and ModE-Sim. Shadings indicate two standard deviations of the ensemble.



336 To analyse how cold the year 1740 really was, we calculated Central European mean temperature in
337 the three data sets. In fact, in ModE-RA, 1740 is the coldest year on record back to 1421 (outside the
338 lower confidence interval of ModE-RA of any year), followed by 1829 (Fig. 9). The coldest 12-month
339 period (not shown) is November 1739 to October 1740. The annual mean temperature of 1740 was
340 2.15 °C below the preindustrial mean (1851-1900). Also shown are CRUTEM5 data in order to
341 extend the climate reconstructions into the present. These data show a warming of 2.5 °C since the
342 preindustrial, such that the cold year 1740 was more than 4 °C cooler than presently.

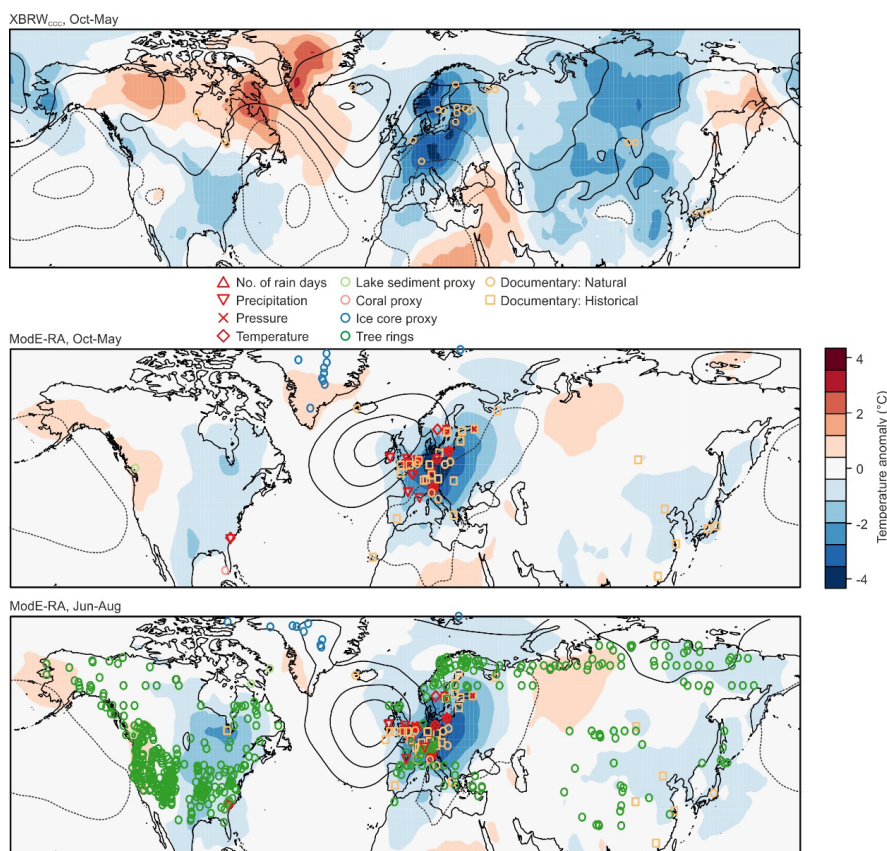
343

344 *A large-scale view*

345 The winter of 1739/40 was not only cold in Europe, but also over North America and Eurasia. This
346 can be seen in a recent reconstruction of cold-season (Oct-May) temperature based only on
347 phenological data (Fig. 10). In fact, 1739/40 was the coldest cold season in the land-area averaged
348 temperature between 35 and 70° N in this reconstruction (which reaches back to 1701, Reichen et al.
349 2022, see Fig. 9, top). The low temperatures in North America are confirmed by a temperature series
350 from Charleston (Fig. 2) that was not included in the reconstruction shown in Fig. 10. In fact, this is
351 also confirmed with documentary data. In North America, the summer of 1740 was cool and wet
352 (Perly, 1891). However, in ModE-RA Siberia is warmer than in XBRW_{CCC}.

353 Documentary data from China show that spring 1740 was late, both in Northern China and in
354 Southern China, with the end date of snow being around 20 days later than average in Beijing-
355 Zhangjiakou region and Nanjing (Xu, 2018; Gong et al., 1983). However, although narrative evidence
356 shows that the winter, especially the late winter, may have been colder than average in southern China
357 (Ding and Zheng, 2017; Zhang, 2004), it was not an extremely cold winter based on existing
358 reconstructions of East Asia (Hao et al., 2018; Wang et al., 2023).

359 The summer (Jun-Aug) temperature anomaly fields are very similar to those of the cold season (Fig.
360 10). One reason might be that for some of the rivers, the thawing takes place only shortly after the
361 start of the warm season assimilation window and these proxies are assimilated both for the cold and
362 warm season. Likewise, since the warm season assimilation window covers Apr-Sep, the tree ring
363 proxies in ModE-RA also affect the Oct-May period. However, the persistence might also be real as it
364 also appears in the analog reconstructions (contours in Fig. 6). Similar as for the cold season, Siberia
365 has also positive temperature anomalies in summer (arguably due to tree rings) such that the annual
366 mean of 1740 was not the coldest year on record in global mean temperature in ModE-RA. Sea-level
367 pressure anomalies show the clear EA pattern over Europe. In addition, they show a positive phase of
368 the Pacific North-American (PNA) pattern, most pronounced in XBRW_{CCC}.



369

370 **Fig. 10.** Anomalies of temperature and sea-level pressure (contour distance 2 hPa centred around zero, negative
371 dashed) for (top) the cold season (Oct-May) 1739/40 in the XBRW_{CCC} data set (Reichen et al., 2022), (middle)
372 the cold season 1739/40 in ModE-RA, and (bottom) summer (Jun-Aug) in ModE-RA, expressed as anomalies
373 from the preceding 30 years. For XBRW_{CCC}, which is based only on phenological data, orange circles mark the
374 locations (displayed with a slight offset if several observations, e.g., freezing and thawing dates, are available
375 from the same location). For ModE-RA, observations entering the data set are also shown.

376

377 *Role of forcings*

378 Finally, we analysed the role of oceanic influences (i.e., NINO3.4 in our case) and of external forcing
379 due to volcanic eruptions. ModE-RA, which is based on the monthly sea-surface temperature
380 reconstructions by Samakinwa et al. (2020), which in turn are based in annual reconstructions by
381 Neukom et al. (2019), show El Niño conditions in 1739 and partly in 1740. To analyse the possible
382 role of El Niño, we performed a correlation analyses, restricting our analysis to the years 1710-2000
383 because of the deteriorating quality further back. Results (Fig. S3) show that almost all correlations
384 for all ensemble members for all indices (NAO in Jan-Feb, EA1 and EA2 in Mar-May) are within
385 ± 0.1 . The strongest (negative) correlations are found for the NAO. The box plots show the spread



386 among the ensemble members, which should not be confounded with the significance of the
387 correlations themselves. In fact, none of the correlations is statistically significant at $p = 0.05$.

388 Another influence could have come from the volcanic eruption of Mount Tarumae, 19-31 Aug 1739.
389 In the volcanic forcing data sets used in ModE-RA as well as in Sigl et al. (2015), this is not a very
390 big eruption, but with a global forcing of -2.4 W m^{-2} exceeds the threshold set in the methods section.
391 We analysed all eruptions with a global forcing stronger than -2 W m^{-2} , again restricting ourselves to
392 the time period 1710-2000 (Fig. S3). We find only weak effects of the eruption, such as a slightly
393 positive response of the NAO in Jan-Feb and positive responses of the EA1 and EA2 pattern.

394

395 **Discussion**

396 *Agreement between data sets and sequence of events*

397 The data sets (ModE-RA and XBRW_{CCC}, but also ModE-RA and the analog reconstruction) agree
398 well with each other, demonstrating that the extremely simple analog approach is suitable for the
399 purpose and that it is possible to study not only climate but also the weather of 1740. Moreover, the
400 findings from the reconstructions are well in line with the documentary evidence.

401 1740 was the coldest year in central Europe since 1421 and the coldest 12-month period was Nov
402 1739 to Oct 1740. The cause for the cold was a specific sequence of events. It started with
403 Scandinavian blocking, which brought cold continental air to Central Europe. Jones and Briffa (2006)
404 address Jan 1740 as a continental high-pressure situation. In our data, this concerns clearly the period
405 5-11 January, while the monthly mean of January as a whole does not show the strongest anomalies
406 over Scandinavia but rather over the UK.

407 During spring (and actually most of the year) the dominant circulation pattern consisted of high
408 pressure or even blocking over the British Isles. This brought cold air from the northern North
409 Atlantic (which at that time of the year is much colder than the European continent) to central Europe.
410 August, then featured cyclonic weather, which brought cold and wet air masses from the West.

411 It is also important to note that the cold began already in autumn 1739 (Fig. S2) and that the following
412 two winters (most notably 1741-42) were also cold. Hence, a multiyear cold period followed a rather
413 mild decade, as pointed out by Jones and Briffa (2006).

414 *Dynamical aspects*

415 The year 1740 started with a negative NAO pattern, which however was not extreme. The cold air
416 outbreak in Jan 1740 is particularly noteworthy as temperature anomalies reached -6 standard
417 deviations. Was this the imprint of a sudden stratospheric warming (SSW)? Obviously, we have no
418 evidence and not even clear indications. SSWs are associated to a collapse of the polar vortex and can
419 affect surface weather for 30-60 days. More frequent cold air outbreaks in Northern Europe are a



420 possible consequence. It is not uncommon that SSWs are preceded by a pressure dipole over Europe
421 (Butler et al., 2017), to which Dec. 1739 bears some resemblance. Everything beyond that, however,
422 would be pure speculation.

423 Following this event, the circulation pattern over Europe took the form of a negative East Atlantic
424 pattern (EA1 or EA2) for a big part of the rest of the year. A similar pattern was also noted for spring
425 by Engel et al. (2013). In ModE-RA, the EA indices in Mar-May reached their most negative state on
426 record and similar for annual means. An existing reconstruction of the NAO and EA in winter
427 (Mellado-Cano et al., 2019), which is however based on only one series, also shows negative
428 anomalies in the winter 1739/40 in both indices.

429 In the Pacific North American sector, we find an anomaly pattern of sea-level pressure that resembles
430 a positive PNA phase. The relatively simple XBRW_{CCC} reconstruction shows this most clearly, but it
431 is also seen in the ModE-RA products.

432 *Role of external forcings*

433 The role of boundary conditions (sea-surface temperatures, land surface) and external forcings can be
434 addressed using ModE-Sim. It shows a cooling in Central Europe of ca. 0.5 °C, i.e., a fraction of the
435 cooling could be due to boundary conditions. In terms of atmospheric circulation, we find a slight
436 negative NAO response in late winter and a very slightly negative EA pattern, but only a small part of
437 the deviations can be explained in that way.

438 In terms of external forcings, the arguably most likely candidate is the eruption of Mount Tarumae,
439 19-31 Aug 1739, which is incorporated in ModE-Sim. This was a highly explosive eruption (VEI=5),
440 but in terms of radiative forcing it was arguably not a very big eruption. It cannot be ruled out that the
441 eruption in the real world was larger, but there is no evidence. It can be stated that Aug 1740 was
442 typical for a volcanic summer, but given the location of Mount Tarumae (Hokkaido, Japan) it is not
443 clear whether an effect is still expected after one year. Analyses of NAO and EA indices with respect
444 to volcanic eruptions in general show only weak effects, which are of opposite sign to what was
445 observed in 1740. We therefore have no indication that the circulation anomalies in 1740 could have
446 been related to a volcanic eruption. Also, solar activity was average in 1740 in the PMIP4 forcings
447 (Jungclauss et al., 2017).

448 *Role of ocean and land surface*

449 In the reconstructions underlying ModE-Sim, 1739/40 were El Niño years. In order to study the
450 possible effect of El Niño on European climate, we performed a simple correlation approach in which
451 we correlated NINO3.4 with indices of NAO, EA1 and EA2. We find slightly negative correlations
452 with NAO in Jan-Feb, which although insignificant, indicate a possible influence. In contrast, for EA1
453 and EA2 in Mar-May we find very small, positive correlations.



454 The reconstructions for 1739/40 are consistent with an El Niño winter. For instance, we see the
455 expected positive PNA response in the cold season 1739/40. Also the negative NAO in Jan-Feb
456 agrees with the correlation analysis and with the literature. El Niño events can lead to a negative,
457 NAO-like response (Brönnimann, 2007), to a weak stratospheric polar vortex and to more frequent
458 SSWs (Domeisen et al., 2019). However, other aspects do not agree. For instance, for the EA1 and
459 EA2 indices we find a positive correlation with NINO3.4 but strongly negative anomalies in 1740.
460 Furthermore, the uncertainty of El Niño reconstructions 300 years ago is high. The reconstruction by
461 Li et al. (2013), for instance, has no clear El Niño event.

462 Other teleconnection mechanisms leading to SSWs and subsequent cold air outbreaks in Europe have
463 been suggested in relation to recent Arctic sea ice decline. The proposed mechanism (Cohen et al.,
464 2014) involves an increase in snow cover over Eurasia in fall due to the low sea ice and increased
465 moisture transport. This could then amplify the planetary wave and lead to a collapse of the
466 stratospheric polar vortex. In order to test the plausibility of such a mechanism in this case we would
467 need to have information on sea ice or snow, which is very scattered for this period. A reconstruction
468 of autumn Barents-Kara Sea ice based on proxies (Zhang et al., 2018) indeed show relatively low sea
469 ice values (compared to the 100 years before and after) around 1740. Indications for slightly cooler
470 and snowy conditions are also found from other records, but they were by no means extreme (see also
471 Reichen et al., 2022).

472 In existing reconstructions, the winter 1739/40 was colder than long-term average only in South
473 China, and in the Yangtze River region, it was colder than past decades but not a cold winter in past
474 centuries (Hao et al., 2018; Hao et al., 2012). However, some of these reconstructions also confirm an
475 even colder winter in East Asia in 1741/42 and 1742/43. Also, the winter 1740/41 was recognized as
476 an extremely cold winter in southern China although not the coldest one based on narrative records
477 (Zheng et al., 2012). Snow cover might have provided a mechanism for the persistence of anomalies
478 over multiple winters (Reichen et al., 2022). However, again, this mechanism remains speculative.

479 *Role of atmospheric internal variability*

480 Finally, we have to address the role of internal atmospheric variability. In our view, after having
481 studied possible forcing factors and after having found no clear indications for external forcings,
482 oceanic or land surface effects, we ascribe most of the anomalous circulation to internal variability (in
483 line with interpretations by Engler et al., 2013, and Jones and Briffa, 2006). Specifically, the record
484 low EA1 and EA2 indices cannot be explained by any of the suggested mechanisms. These were
485 however, dominating the cold of the year 1740.

486 **Conclusions**

487 The year 1740 was arguably the coldest in Central Europe since 1421. The annual mean temperature
488 was 2 °C below pre-industrial levels, and the extended cold season 1739/40 was also the coldest one



489 for the northern midlatitude land mass since 1700. The winter of 1739/40 and the cold year of 1740
490 had severe consequences for societies in Europe, including increased prices and famine. It is therefore
491 relevant to assess the chain of processes causing such a cold year. Still even this large excursion of
492 climate dwarfs against changes observed in the last 120 years.

493 The analysis revealed that the coldness was due to the special sequence of events, i.e., a continental
494 high/Scandinavian blocking in January, then negative East Atlantic pattern during spring, a cyclonic
495 summer, and again negative EA pattern. Most of this is arguably due to internal atmospheric
496 variability. We studied many possible forcings and system effects and found no clear indications for a
497 forced signal. Only the circulation anomalies in January might have been made more likely by a
498 possible El Niño event, or, even much more speculative, low Arctic sea ice and increased snow cover.
499 Furthermore, part of the general cooling over Europe can be explained by a volcanic eruption in 1739.
500 However, this explains only a small fraction, and the most outstanding feature of this climatic
501 anomaly, the negative East Atlantic pattern that persisted for almost a year, shows no indication of a
502 forced contribution.

503 The analysis shows that extreme internal variability of the atmosphere is possible. It also shows that
504 daily weather data and a new monthly climate reconstruction together allow a detailed insight into the
505 mechanisms that brought forth a momentous climate event that happened close to 300 years back in
506 the past.

507

508 **Data availability statement:** The ModE-RA, ModE-RAclim, and ModE-Sim data (Valler et al., 2024) can be
509 downloaded from DKRZ (<https://www.wdc-climate.de/ui/entry?acronym=ModE-RA>). ERA5 reanalysis data are
510 available from the Copernicus Climate Change Service Data Store. XBRW_{CC} data are available from
511 PANGAEA (Reichen et al., 2022, <https://doi.pangaea.de/10.1594/PANGAEA.934288>), CRUTEM5 is available
512 from <https://crudata.uea.ac.uk/cru/data/temperature/> (accessed 4 Mar 2024). The historical station data are
513 available from figshare (doi:10.6084/m9.figshare.25879186). The St. Blaise data were taken from EURO-
514 CLIMHIST (Pfister et al., 2017, <https://www.euroclimhist.unibe.ch/>, accessed 4 Mar 2024).

515 **Code availability statement:** All analyses were done in R using standard code. The ModE-RA family of
516 products can be accessed through and all corresponding analyses can also be done at the website: <https://mode->
517 [ra.unibe.ch/climeapp/](https://mode-ra.unibe.ch/climeapp/).

518 **Author contributions:** SB performed the analyses, JF and SC provided historical observations and
519 documentary sources, LP provided the weather type reconstructions. All authors contributed to writing the
520 paper.

521 **Funding Information:** The work was funded by the Swiss National Science Foundation projects Wear
522 (188701) and DVDW (219746) and the European Commission through H2020 (ERC Grant PALAEO-RA
523 787574) and the National Science Centre, Poland project No. 2020/37/B/ST10/00710.

524 **Competing interests.** The contact author has declared that none of the authors has any competing interests.

525 **Acknowledgements.** We would like to thank Yuri Brugnara, Dario Camuffo, Daniel Rousseau, Richard Cornes,
526 and Rolando Garcia-Herrera for providing the pressure and wind data. The simulations underlying ModE-RA
527 were performed at the Swiss Supercomputer Centre (CSCS).



528 **References**

- 529 Barnston, A. G., and Livezey, R. E.: Classification, Seasonality and Persistence of Low-Frequency Atmospheric
530 Circulation Patterns. *Mon. Wea. Rev.*, 115, 1083–1126, 1987.
- 531 Barriopedro, D., Gallego, D., Álvarez-Castro, M. C., García-Herrera, R., Wheeler, D., Peña-Ortiz, C., and
532 Barbosa, S. M.: Witnessing North Atlantic westerlies variability from ships' logbooks (1685–2008). *Clim.
533 Dyn.*, 43, 939–955, 2014.
- 534 Bergström, H. and Moberg, A.: Daily air temperature and pressure series for Uppsala (1722–1998). *Clim.
535 Change*, 53, 213–252, 2002.
- 536 Brönnimann, S.: Impact of El Niño–Southern Oscillation on European climate. *Rev. Geophys.*, 45, RG3003,
537 2007.
- 538 Brönnimann, S. Allan, R., Ashcroft, L., Baer, S., Barriendos, M., Brázdil, R., Brugnara, Y., Brunet, M.,
539 Brunetti, M., Chimani, B., Cornes, R., Domínguez-Castro, F., Filipiak, J., Founda, D., García Herrera, R.,
540 Gergis, J., Grab, S., Hannak, L., Huhtamaa, H., Jacobsen, K. S., Jones, P., Jourdain, S., Kiss, A., Lin, K. E.,
541 Lorrey, A., Lundstad, E., Luterbacher, J., Mauelshagen, F., Maugeri, M., Maughan, N., Moberg, A., Neukom,
542 R., Nicholson, S., Noone, S., Nordli, Ø., Ólafsdóttir, K. B., Pearce, P. R., Pfister, L., Pribyl, K., Przybylak, R.,
543 Pudmenzky, C., Rasol, D., Reichenbach, D., Řezníčková, L., Rodrigo, F. S., Rohde, R., Rohr, C., Skrynyk,
544 O., Slonosky, V., Thorne, P., Valente, M. A., Vaquero, J. M., Westcott, N. E., Williamson, F., and
545 Wyszynski, P.: Unlocking pre-1850 instrumental meteorological records: A global inventory, *B. Am.
546 Meteorol. Soc.*, 100, ES389–ES413, 2019.
- 547 Brönnimann, S. and Brugnara, Y.: The weather diaries of the Kirch family: Leipzig, Guben, and Berlin, 1677–
548 1774. *Clim. Past*, 19, 1435–1445, <https://doi.org/10.5194/cp-19-1435-2023>, 2023.
- 549 Butler, A. H., Sjöberg, J. P., Seidel, D. J., and Rosenlof, K. H.: A sudden stratospheric warming compendium,
550 *Earth Syst. Sci. Data*, 9, 63–76, <https://doi.org/10.5194/essd-9-63-2017>, 2017.
- 551 Camuffo, D., and Jones, P.: Improved understanding of past climatic variability from early daily European
552 instrumental sources. *Climatic Change*, 53, 1–4, 2002, <https://doi.org/10.1023/A:1014902904197>
- 553 Cohen, J., Screen, J., Furtado, J., Barlow, M., Whittleston, D., Coumou, D., Francis, J., Dethloff, K., Entekhabi,
554 D., Overland, J., and Jones, J.: Recent Arctic amplification and extreme mid-latitude weather. *Nature Geosci.*,
555 7, 627–637, 2014, <https://doi.org/10.1038/ngeo2234>
- 556 Cornes R. C., Jones, P. D., Briffa, K. R., and Osborn, T. J.: A daily series of mean sea-level pressure for
557 London, 1692–2007. *Int. J. Climatol.*, 32, 641–656, 2012.
- 558 Cornes, R. C., Jones, P. D., Brandsma, T., Cendrier, D., and Jourdain, S. (2023) The London, Paris and De Bilt
559 sub-daily pressure series. *Geoscience Data Journal*, 00, 1–12. Available from:
560 <https://doi.org/10.1002/gdj3.226>
- 561 Dickson, D.: *Arctic Ireland: The Extraordinary Story of the Great Frost and Forgotten Famine of 1740–1741*,
562 Whiterow Press, Belfast, 1997.
- 563 Ding, L. and Zheng, J.: Reconstruction and characteristics of series of winter cold index in South China in the
564 past 300 years. *Geographical Research*, 36, 1183–1189, <https://doi.org/10.11821/dlyj201706015>, 2017.
- 565 Domeisen, D. I., Garfinkel, C. I., and Butler, A. H.: The teleconnection of El Niño Southern Oscillation to the
566 stratosphere. *Rev. Geophys.*, 57, 5–47, <https://doi.org/10.1029/2018RG000596>, 2019.
- 567 Engler, S., Mauelshagen, F., Werner, J., and Luterbacher, J.: The Irish famine of 1740–1741: famine
568 vulnerability and "climate migration", *Clim. Past*, 9, 1161–1179, <https://doi.org/10.5194/cp-9-1161-2013>,
569 2013.
- 570 Filipiak, J., Przybylak, R., and Oliński, P.: The longest one-man weather chronicle (1721–1786) by Gottfried
571 Reyger for Gdańsk, Poland as a source for improved understanding of past climate variability. *Int. J.
572 Climatol.*, 39, 828–842, doi: 10.1002/joc.5845, 2019.
- 573 Gillespie, T.: The great Irish frost of winter 1739–40 in Mayo recalled. *The Connaught Telegraph*, 30 December
574 1939 (<https://www.con-telegraph.ie/2022/12/31/the-great-irish-frost-of-winter-1739-40-in-mayo-recalled/>)



- 575 Gong, G., Zhang, P., and Zhang, J.: A study on the climate of the 18th century of the lower Changjiang valley in
576 China. *Geographical Research*, 2, 20-33, <https://doi.org/10.11821/yj1983020003>, 1983.
- 577 Hao, Z. X., Zheng, J. Y., Ge, Q. S. and Wang, W. C.: Winter temperature variations over the middle and lower
578 reaches of the Yangtze River since 1736 AD. *Clim. Past*, 8, 1023–1030, 2012.
- 579 Hao, Z., Yu, Y., Ge, Q. and Zheng, J.: Reconstruction of high-resolution climate data over China from rainfall
580 and snowfall records in the Qing Dynasty. *WIREs Clim Change*, 9, e517, 2018.
- 581 Hersbach, H., Bell, B., Berrisford, P., Hirahara, S., Horányi, A., Muñoz-Sabater, J., Nicolas, J., Peubey, C.,
582 Radu, R., Schepers, D., Simmons, A., Soci, C., Abdalla, S., Abellan, X., Balsamo, G., Bechtold, P., Biavati,
583 G., Bidlot, J., Bonavita, M., De Chiara, G., Dahlgren, P., Dee, D., Diamantakis, M., Dragani, R., Flemming,
584 J., Forbes, R., Fuentes, M., Geer, A., Haimberger, L., Healy, S., Hogan, R. J., Hólm, E., Janisková, M.,
585 Keeley, S., Laloyaux, P., Lopez, P., Lupu, C., Radnoti, G., de Rosnay, P., Rozum, I., Vamborg, F., Villaume,
586 S., and Thépaut, J.-N.: The ERA5 global reanalysis. *Q. J. R. Meteorol. Soc.*, 146, 1999–2049, 2020.
587 <https://doi.org/10.1002/qj.3803>
- 588 Jones, P. D., and Briffa, K.R.: Unusual Climate in Northwest Europe During the Period 1730 to 1745 Based on
589 Instrumental and Documentary Data. *Clim. Change* 79, 361–379 (2006). [https://doi.org/10.1007/s10584-006-](https://doi.org/10.1007/s10584-006-9078-6)
590 [9078-6](https://doi.org/10.1007/s10584-006-9078-6)
- 591 Jungclauss, J. H., Bard, E., Baroni, M., Braconnot, P., Cao, J., Chini, L. P., Egorova, T., Evans, M., González-
592 Rouco, J. F., Goosse, H., Hurrett, G. C., Joos, F., Kaplan, J. O., Khodri, M., Klein Goldewijk, K., Krivova, N.,
593 LeGrande, A. N., Lorenz, S. J., Luterbacher, J., Man, W., Maycock, A. C., Meinshausen, M., Moberg, A.,
594 Muscheler, R., Nehrbass-Ahles, C., Otto-Bliesner, B. I., Phipps, S. J., Pongratz, J., Rozanov, E., Schmidt, G.
595 A., Schmidt, H., Schmutz, W., Schurer, A., Shapiro, A. I., Sigl, M., Smerdon, J. E., Solanki, S. K.,
596 Timmreck, C., Toohey, M., Usoskin, I. G., Wagner, S., Wu, C.-J., Yeo, K. L., Zanchettin, D., Zhang, Q., and
597 Zorita, E.: The PMIP4 contribution to CMIP6 – Part 3: The last millennium, scientific objective, and
598 experimental design for the PMIP4 past1000 simulations, *Geosci. Model Dev.*, 10, 4005–4033,
599 <https://doi.org/10.5194/gmd-10-4005-2017>, 2017.
- 600 Lamb, H. H. Britain's Changing Climate. *The Geographical Journal*, 133, 445-466,
601 <https://doi.org/10.2307/1794473>, 1967.
- 602 Li, J., Xie, S.-P., Cook, E. R., Morales, M. S., Christie, D. A., Johnson, N. C., Chen, F., D'Arrigo, R., Fowler, A.
603 M., Gou, X. and Fang, K.: El Niño modulations over the past seven centuries. *Nature Climate Change*, 3,
604 822–826, [10.1038/nclimate1936](https://doi.org/10.1038/nclimate1936), 2013.
- 605 Lundstad, E., Brugnara, Y., Pappert, D., Kopp, J., Hürzeler, A., Andersson, A., Chimani, B., Cornes, R.,
606 Demarée, G., Filipiak, J., Gates, L., Ives, G. L., Jones, J. M., Jourdain, S., Kiss, A., Nicholson, S. E.,
607 Przybylak, R., Jones, P. D., Rousseau, D., Tinz, B., Rodrigo, F. S., Grab, S., Domínguez-Castro, F.,
608 Slonosky, V., Cooper, J., Brunet, N. and Brönnimann, S.: Global historical climate database - HCLIM.
609 *Scientific Data*, 10, 44, 2023.
- 610 Luterbacher, J., Xoplaki, E., Dietrich, D., Rickli, R., Jacobeit, J., Beck, C., Gyalistras, D., Schmutz, C., and
611 Wanner, H.: Reconstruction of Sea Level Pressure fields over the Eastern North Atlantic and Europe back to
612 1500, *Clim. Dynam.*, 18, 545–561, 2002.
- 613 Manley, G.: The Great Winter of 1740. *Weather* 14, 11–17, 1957.
- 614 Mellado-Cano, J., Barriopedro, D., García-Herrera, R., Trigo, R. M., and Hernández, A.: Examining the North
615 Atlantic Oscillation, East Atlantic Pattern, and Jet Variability since 1685. *J. Clim.*, 32, 6285–6298,
616 <https://doi.org/10.1175/JCLI-D-19-0135.1>, 2019.
- 617 Neukom, R., Steiger, N., Gómez-Navarro, J.J. Wang, J., Werner, J. P.: No evidence for globally coherent warm
618 and cold periods over the preindustrial Common Era. *Nature*, 571, 550–554, [https://doi.org/10.1038/s41586-](https://doi.org/10.1038/s41586-019-1401-2)
619 [019-1401-2](https://doi.org/10.1038/s41586-019-1401-2), 2019.
- 620 Osborn, T. J. et al. Land surface air temperature variations across the globe updated to 2019: the CRUTEM5
621 dataset. *J. Geophys. Res.* 126, e2019JD032352, 2021.



- 622 Pappert, D., Barriendos, M., Brugnara, Y., Imfeld, N., Jourdain, S., Przybylak, R., Rohr, C. and Brönnimann, S.:
623 Statistical reconstruction of daily temperature and sea-level pressure in Europe for the severe winter 1788/9.
624 *Clim. Past*, 18, 2545–2565, 2022.
- 625 Perley, S.: *Historic Storms of New England*. Salem Press Publishing and Printing Company, 1891.
- 626 Pfister C., and Wanner H.: *Climate and Society in Europe*. Bern: Haupt Verlag, 2021.
- 627 Pfister, C., Rohr, C., and Jover, A. C. C.: Euro-Climhist: eine Datenplattform der Universität Bern zur Witterungs-,
628 Klima- und Katastrophengeschichte. *Wasser Energie Luft*, 109, 45–48, 2017.
- 629 Pfister, L., Wilhelm, L., Brugnara, Y., Imfeld, N., Brönnimann, S.: Weathertype Reconstruction using Machine
630 Learning Approaches. *EGUsphere* [preprint], 2024, <https://doi.org/10.5194/egusphere-2024-1346>.
- 631 Post, J. D.: Climatic variability and the European mortality wave of the early 1740s, *J. Interdiscipl. Hist.*, 15, 1–
632 30, 1984.
- 633 Reichen, L., Burgdorf, A.-M., Brönnimann, S., Rutishauser, M., Franke, J., Valler, V., Samakinwa, E., Hand,
634 R., and Brugnara, Y.: A Decade of Cold Eurasian Winters Reconstructed for the Early 19th Century. *Nature*
635 *Communications*, 13, 2116, <https://doi.org/10.1038/s41467-022-29677-8>, 2022.
- 636 Rousseau, D.: Le cahier d'observations météorologiques de Réaumur. Ses mesures de températures de 1732 à
637 1757. *La Météorologie*, 105, 21–28, 2019.
- 638 Samakinwa, E., Valler, V., Hand, R., Neukom, R., Gómez-Navarro, J. J., Kennedy, J., Rayner, N. A. and
639 Brönnimann, S.: An ensemble reconstruction of global monthly sea surface temperature and sea ice
640 concentration 1000–1849. *Scientific Data*, 8, 261, 2021.
- 641 Sigl, M., Winstrup, M., McConnell, J. R., Welten, K. C., Plunkett, G., Ludlow, F., Büntgen, U., Caffee, M.,
642 Chellman, N., Dahl-Jensen, D., Fischer, H., Kipfstuhl, S., Kostick, C., Maselli, O. J., Mekhaldi, F.,
643 Mulvaney, R., Muscheler, R., Pasteris, D. R., Pilcher, J. R., Salzer, M., Schüpbach, S., Steffensen, J. P.,
644 Vinther, B. M., and Woodruff, T. E.: Timing and climate forcing of volcanic eruptions for the past 2,500
645 years. *Nature*, 523, 543–549, 2015.
- 646 Société Météorologique de France: *Annuaire de la Société Météorologique de France*, 14, 1866.
- 647 Titchner, H. A. and Rayner, N. A.: The Met Office Hadley Centre sea ice and sea surface temperature data set,
648 version 2: 1. Sea ice concentrations. *J. Geophys. Res.*, 119, 2864–2889, doi: 10.1002/2013JD020316, 2014.
- 649 Valler, V., Franke, J., Brugnara, Y., and Brönnimann, S.: An updated global atmospheric paleo-reanalysis
650 covering the last 400 years. *Geosc. Data J.*, 9, 89–107, doi: 10.1002/gdj3.121, 2022.
- 651 Valler, V., Franke, J., Brugnara, Y., Samakinwa, E., Hand, R., Burgdorf, A.-M., Lipfert, L., Friedman, A.,
652 Lundstad, E., and Brönnimann, S.: ModE-RA - a global monthly paleo-reanalysis of the modern era (1421–
653 2008). *Scientific Data*, 11, 36, <https://doi.org/10.1038/s41597-023-02733-8>, 2024.
- 654 Wang, J., Yang, B., Wang, Z., Luterbacher, J. and Ljungqvist, F. C.: Recent weakening of seasonal temperature
655 difference in East Asia beyond the historical range of variability since the 14th century. *Sci. China Earth Sci.*,
656 66, 1133–1146, <https://doi.org/10.1007/s11430-022-1066-5>, 2023.
- 657 Xu, Q.: Analysis of temperature and snow characteristics in winter in Beijing and Zhangjiakou region, Master
658 thesis, Agronomy College, Shenyang Agricultural University, China, 2017.
- 659 Zhang, D.: *A compendium of Chinese meteorological records of the last 3,000 years*. Phoenix House. Ltd.,
660 2013.
- 661 Zhang, Q., Xiao, C. D., Ding, M. H., and Dou T. F.: Reconstruction of autumn sea ice extent changes since
662 AD1289 in the Barents-Kara Sea, Arctic. *Science China Earth Sciences*, <https://doi.org/10.1007/s11430-017-9196-4>, 2018.
- 664 Zheng, J. Y., Ding, L. L., Hao, Z. X. and Ge, Q. S.: Extreme cold winter events in southern China during AD
665 1650–2000. *Boreas*, 41, 1–12, 2012.